Status of dynamic diagnostics of plasma material interaction based on synchrotron radiation scattering at the VEPP-4 beamline 8

Arakcheev A.S.[1,2,3], Ancharov A.I.[4], Aulchenko V.M.[1], Bugaev S.V.[1], Burdakov A.V.[1,3], Chernyakin A.D.[1], Evdokov O.V.[4], Kasatov A.A.[1], Kosov A.V.[1], Piminov P.A.[1], Polosatkin S.V.[1,3], Popov V.A.[1,2], Sharafutdinov M.R.[1,4], Shekhtman L.I.[1], Shmakov A.N.[5], Shoshin A.A.[1,2], Skovorodin D.I.[1], Tolochko B.P.[1,4], Vasilyev A.A.[1], Vyacheslavov L.N.[1,2], Zhulanov V.V.[1]

[1] Budker Institute of Nuclear Physics SB RAS
[2] Novosibirsk State University
[3] Novosibirsk State Technical University
[4] Institute of Solid State Chemistry and Mechanochemistry SB RAS
[5] Boreskov Institute of Catalysis SB RAS

Synchrotron and Free electron laser Radiation: generation and application (SFR-2016), 06.07.2016

Motivation

Fusion reactor

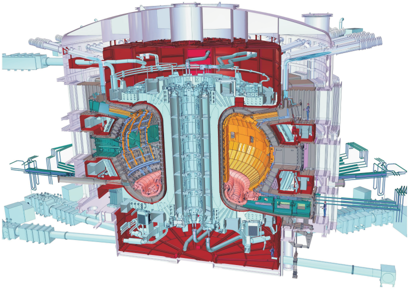

ITER drawing

- Plasma volume: $837m^3$.
- Fusion power: $\sim$ 500MW.
- Plasma pulse time: $\sim$ 3000s.
- First plasma data: 2025.
- Strong erosion of the first wall and divertor plates under powerful plasma flow.

Conditions at the first wall

- Ion flow: 10^{24}ion/m^{2}s,
- Fusion neutron flow: 10^{13}neutron/m^{2}s,
- Thermal loads:
  - Permanent: $40 - 60$MW/m^2,
  - Edge localized mods (ELM): ~ 10MJ/m^2 during $0.1 - 1$ms,
  - Thermal quench: ~ 150MJ/m^2 during $1 - 5$ms,
  - Runaway electrons: ~ 30MJ/m^2.

Material erosion and degradation

- Sputtering:
  - Physical sputtering,
  - Chemical sputtering.
- Evaporation,
- Surface and structure modifications (including DPA and recrystallization),
- Impurities retention (including α-particles):
  - Bubble growth,
  - Blistering,
  - Flaking,
  - "Fuzz" growth.
- Brittle destruction:
  - Cracking,
  - Dust particles formation and ejection.
- Melting and flowing away,
- Boiling and splashing.

The most promising materials: W, C, Be, Li.

Overview of *ex-situ* studies

Recrystallization

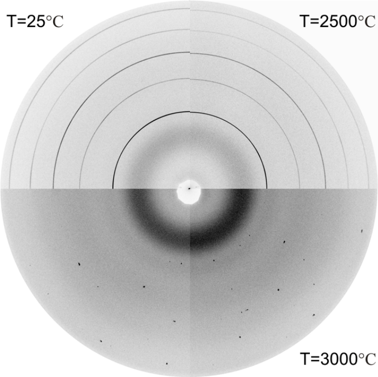

Diffraction on tungsten wire at station "Diffractometry in hard X-rays"

- The growth of the material grains significantly spoils the material properties.
- 2D detector was used to measure the average grain size.
- Tungsten-molybdenum composite material for the recrystallisation preventing was tested.
- Current status: measurements are completed, data analysis is in progress.

Dissolved impurities

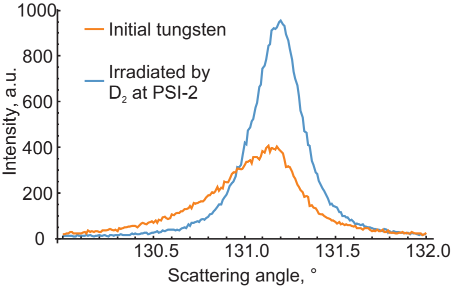

Diffraction peaks measured at station “Precision diffractometry and anomalous scattering”

- The dissolved in metals impurities could lead to embrittlement and several specific types of erosion.
- The change of the diffraction peaks at irradiated tungsten was detected.
- Current status: much more experiments and interpretations should be done to understand something.

Modification of material structure

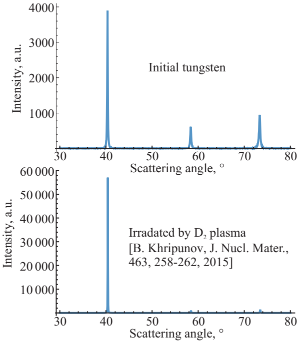

Diffraction peaks measured at station "Precision diffractometry and anomalous scattering"

- The strong change of the diffraction intensity and the ratio of the different peaks intensity are measured.
- The orientation of the irradiated surface layer could significantly change the material properties.
- Possible explanation: the columnar structure of molten and crystallized tungsten.

Residual stresses and deformations

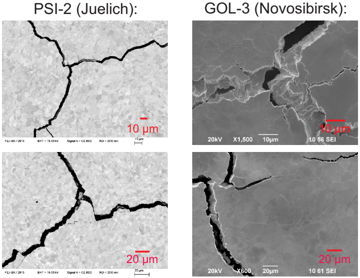

Cracks on the tungsten after pulsed heat loads

- The periodical pulsed ejections of the plasma to divertor plates are expected during the standard operation regime.
- The cracks causes the overheating, dust particle formation, intensify material retention, etc.
- The pulsed heat loads are reason of the tungsten cracking.
- The mechanical stress causing the cracking appears due to plastic deformation of the material.

Residual stresses and deformations

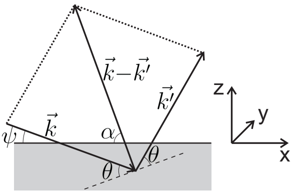

Diffraction scheme

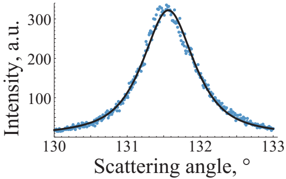

Diffraction peak

- The variation of the sample orientation changes the SR scattering angle due to residual deformation.
- Geometry:
  $n_x = \cos\alpha\cos\phi = \sin(\psi-\theta)\cos\phi,$
  $n_y = \cos\alpha\sin\phi = \sin(\psi-\theta)\sin\phi,$
  $n_z = \sin\alpha = \cos(\psi-\theta).$
- Effect:

$$\frac{1}{\sin\theta} = \frac{2(d_0+\delta d)}{n\lambda} = \frac{2d_0}{n\lambda}(1- u_{xx}\sin^2(\psi-\theta)\cos^2\phi - u_{yy}\sin^2(\psi-\theta)\sin^2\phi - u_{zz}\cos^2(\psi-\theta) - 2u_{xy}\sin^2(\psi-\theta)\cos\phi\sin\phi - 2u_{xz}\sin(\psi-\theta)\cos(\psi-\theta)\cos\phi - 2u_{yz}\sin(\psi-\theta)\cos(\psi-\theta)\sin\phi).$$

Residual stresses and deformations

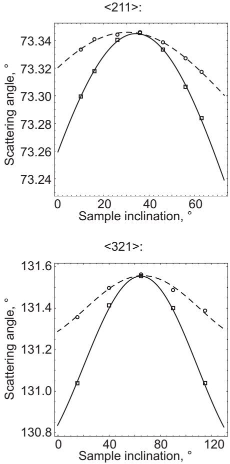

- The variation of the sample orientation changes the SR scattering angle due to residual deformation.
- Geometry:
  $n_x = \cos\alpha\cos\phi = \sin(\psi-\theta)\cos\phi,$
  $n_y = \cos\alpha\sin\phi = \sin(\psi-\theta)\sin\phi,$
  $n_z = \sin\alpha = \cos(\psi-\theta).$
- Effect:

$$\frac{1}{\sin\theta} = \frac{2(d_0+\delta d)}{n\lambda} = \frac{2d_0}{n\lambda}(1- u_{xx}\sin^2(\psi-\theta)\cos^2\phi - u_{yy}\sin^2(\psi-\theta)\sin^2\phi - u_{zz}\cos^2(\psi-\theta) - 2u_{xy}\sin^2(\psi-\theta)\cos\phi\sin\phi - 2u_{xz}\sin(\psi-\theta)\cos(\psi-\theta)\cos\phi - 2u_{yz}\sin(\psi-\theta)\cos(\psi-\theta)\sin\phi).$$

Residual stresses and deformations

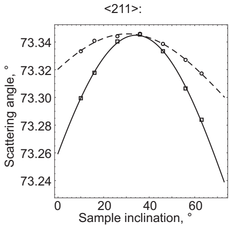

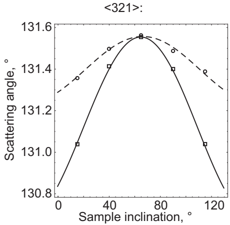

Table: Components of the deformation and stress tensors.

	<211>	<321>
u_{xx}	$2.22 \cdot 10^{-3}$	$2.44 \cdot 10^{-3}$
u_{yy}	$0.2 \cdot 10^{-3}$	$0.22 \cdot 10^{-3}$
u_{zz}	$-0.94 \cdot 10^{-3}$	$-1.04 \cdot 10^{-3}$
u_{xz}	$0.13 \cdot 10^{-3}$	$0.05 \cdot 10^{-3}$
u_{yz}	$0.13 \cdot 10^{-3}$	$-0.02 \cdot 10^{-3}$
σ_{xx}, MPa	1010	1115
σ_{yy}, MPa	364	403
σ_{xz}, MPa	42	15
σ_{yz}, MPa	40	5

Axis x is the rolling direction.

Residual stresses and deformations

In the case of thin heated area there are simple expressions for elastic stresses and deformations:

$$u_x^e = u_y^e = 0,$$

$$u_{zz}^e = \frac{1-\sigma}{1+\sigma}\alpha\left(T(z) - T_0\right),$$

$$\sigma_{zz}^e = \sigma_{xy}^e = \sigma_{xz}^e = \sigma_{yz}^e = 0,$$

$$\sigma_{xx}^e = \sigma_{yy}^e = -\frac{\alpha E(T(z) - T_0)}{(1-\sigma)},$$

where $\vec{u}^e$ is the elastic displacements, σ_{ij}^e is the stress tensor,
α is the linear thermal extension coefficient, E is the Young's modulus, σ is the Poisson's ratio, T is the temperature., T_0 is the initial temperature.
Axis z is perpendicular to the surface,
x and y are parallel to the surface.

In-situ experiments

In-situ experiments

Fast processes during plasma irradiation:

- Deformation during pulsed heat load,
- Recrystallization during pulsed heat load,
- Hydrogen and helium retention and diffusion.

Why did we choose deformation during pulsed heat load for first experiments?

- The measured residual effects,
- Well-understood theoretical description,
- Easy experimental simulation.

Initial conditions

SR sources VEPP-3 and VEPP-4

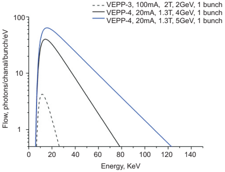

SR spectrum

1D X-ray detector

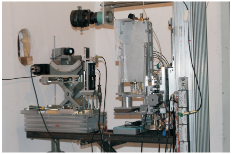

Channel width: 100μm

Model of deformation

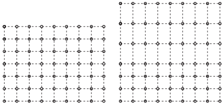

The deformation of crystal structure

Pulsed heat load simulation

Laser:

- Energy: 1J,
- Duration: 140μs,
- Wavelength: 1064nm.

Requirements to the measurements

- Dynamical measurements during pulsed heating,
- Measurements inside material,
- Spacial resolution inside material.

Restrictions to scheme of experiment

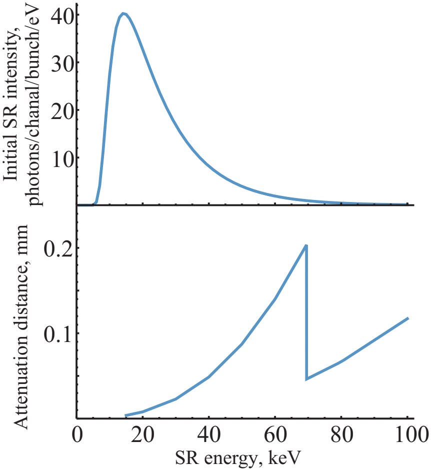

1. SR energy: 69keV

Restrictions to scheme of experiment

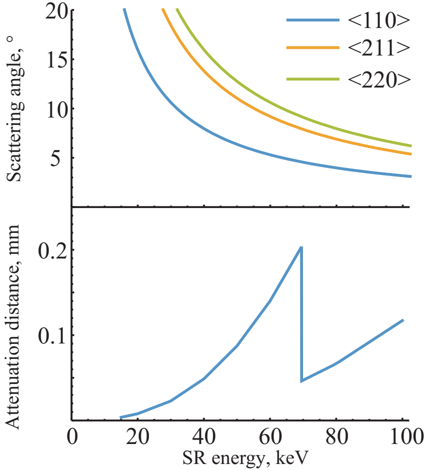

1. SR energy: 69keV

Restrictions to scheme of experiment

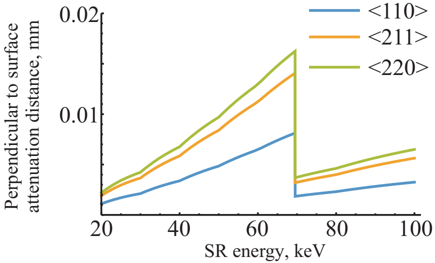

1. SR energy: 69keV
2. Laue diffraction

Restrictions to scheme of experiment

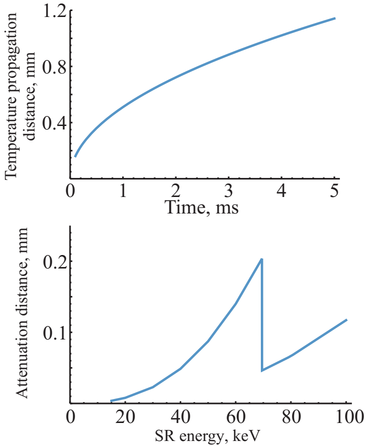

1. SR energy: 69keV
2. Laue diffraction
3. Single crystal

Restrictions to scheme of experiment

Channel width of the 1D detector: 100μm.
Typical shift at the parallel scattering: 10μm.

1. SR energy: 69keV
2. Laue diffraction
3. Single crystal
4. Diverging diffracted SR

The effect causing the divergence of the diffracted SR is necessary for spatial resolution!

Scheme of experiment

Basic variant:

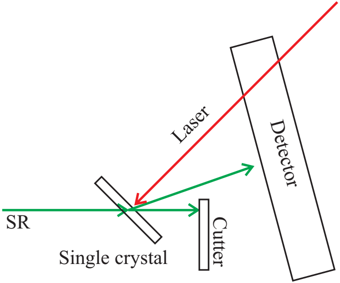

- The deep penetration into material.
- Spatial resolution.
- Thin samples.

Reserve variant:

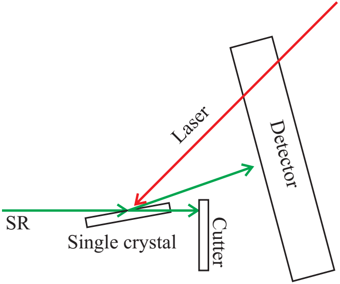

- Single crystal surface.
- Only surface measurements.

Scheme of experiment

Basic variant:

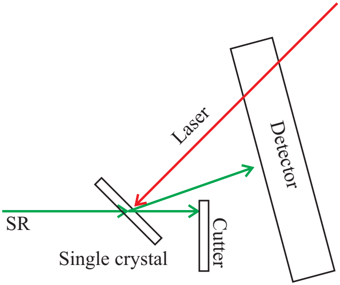

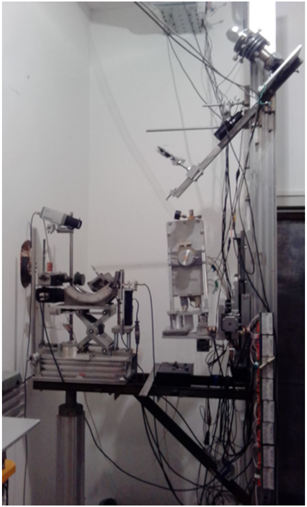

"Diverging" effect

Rotation of crystal planes at the heating of the surface layer:

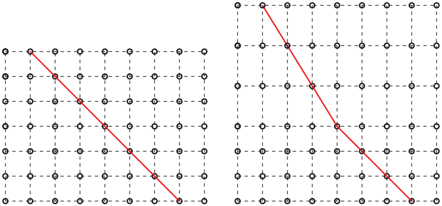

- Compression or expansion of the surface layer result in rotation of the "reflecting" crystal plane.
- $\delta 2\theta \sim \sin(2\alpha)$
- The variation of the scattering angle changes the energy of the diffracted SR. It makes possible to use the sharp change of the intensity near K-egde.

“Diverging” effect

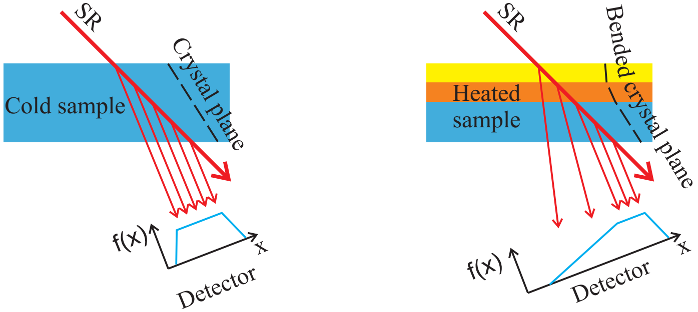

The distribution of the deformations can be calculated using the shape of the diffraction peak.

What did we expect?

Experiment parameters:

- SR cross-section: 2mm × 2mm.
- Laser diameter: 1mm.
- Laser energy: 1J.
- Laser duration: 140μs.
- Temporal resolution: 20μs.
- Single crystal thickness: 250μm.
- Distance to detector: 300mm.
- Geometry:

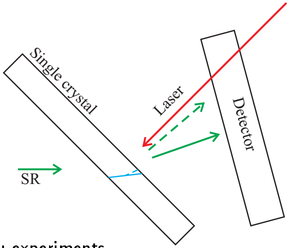

Consequences:

- Temperature propagation distance during irradiation: 200μm.
- Heating up to 500°C.
- Expected effect: $\delta 2\theta = \frac{1+\sigma}{4}\alpha(T - T_0) \approx 0.7\text{mrad} \approx 0.04°$.
- Detector channel width: $1\text{channel} = 100\mu\text{m} \approx 0.3\text{mrad} \approx 0.02°$.
- The method of the taking into account plastic deformation is under discussion.

First results

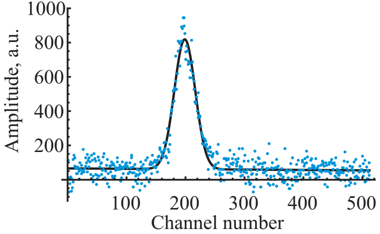

Frame obtained during 20μs.

- Frames number: 30.
- Channel number: 512.
- Frame duration: from 25ns to 200μs.

First results

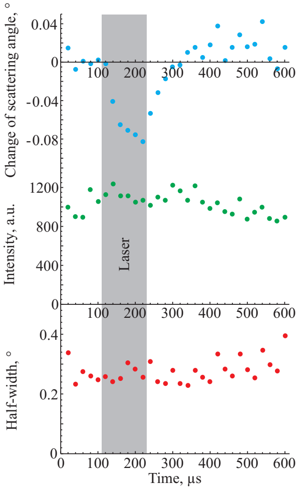

- The scattering angle changes during laser heating and quickly returns back.
- The intensity of the scattered SR and the width of the diffraction peak do not change significantly.

Bending of crystal

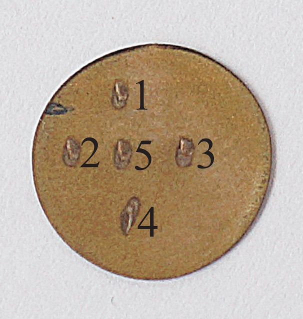

- 1, 2, 3, 4, 5 – laser heating.
- 5 – SR.

Bending of crystal

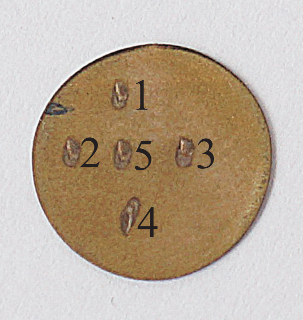

1. 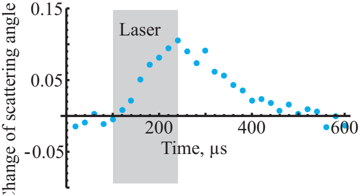

2. No effect.
3. No effect.
4. 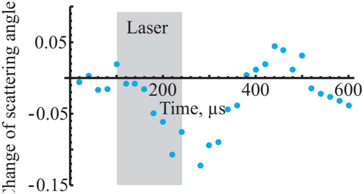

Bending of crystal

- The bending is result of the small thickness of the sample.
- The bending does not correspond to real situation at the first wall in fusion reactor.
- The thicker samples will be used at next experiments.
- We tried to prove the effect of the crystal plane rotation.

Crystal plane rotation

- The direction of the bending could be changes, while the direction of the crystal plane rotation always is positive.
- The bending is proportional to temperature gradient, while the crystal plane rotation is proportional to the temperature.

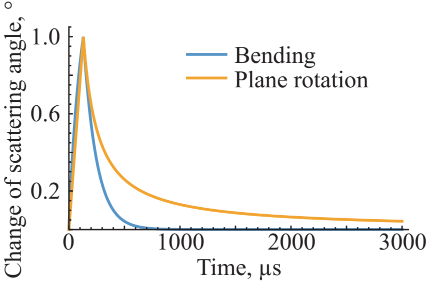

Crystal plane rotation

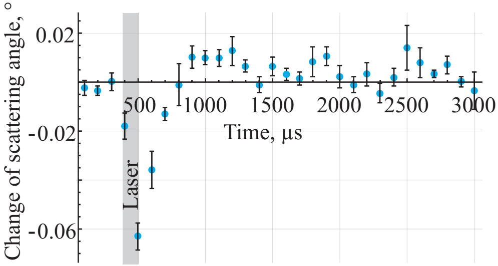

- The reverse of the scattering angle change was measured.

Crystal plane rotation

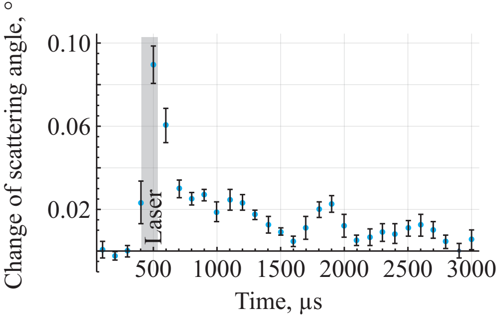

- The SR beam cross-section was decreased to be smaller than laser cross-section.

Crystal plane rotation

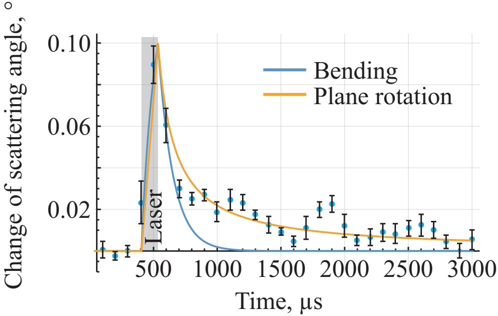

- The rotation of the crystal plane fits experimental results better than bending.

Diffraction peak shape

Diffraction peak before irradiation

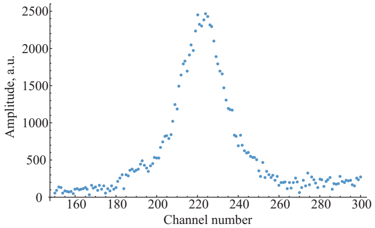

Diffraction peak during irradiation

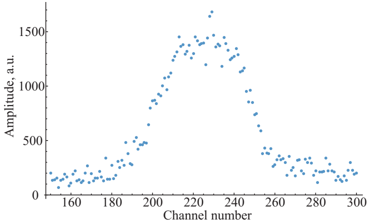

The diffraction peak shape processing is in progress.

Conclusions

Facility

Operable:

- Goniometers.
- Gas 1D X-ray detector .
- 1J laser.

Under construction:

- Silicon 1D X-ray detector.
- 100J laser.
- Pirometer.
- Vacuum vessel.

Theory and mathematical processing

Done:

- Proved rotation of crystal plane during pulsed heating

In progress:

- Analysis of diffraction peak shape to calculate stress and deformation distributions

Main result

The fast *in-situ* X-ray diffractometry of solid is demonstrated.

Thank you for attention